

Communication

Rapid Synthesis of Citric Acid Coated Manganese Ferrite Nanoparticles: Electrochemical Supercapacitor Applications

Palem Vishnu Vardhan^{1,*} , Pichumani Moorthi² , Palanivel Nihitha¹ ,
Sivakumar Kamalikka¹ , Karthikeyan Surya¹ 

¹Department of Biomedical Engineering, Sri Ramakrishna Engineering College, Coimbatore, India

²Department of Nanoscience and Technology, Sri Ramakrishna Engineering College, Coimbatore, India

Abstract

To manufacture nanoscale materials with high surface density, achieving average pore size and volume requires energy-intensive and time-consuming operations. We present a straightforward rapid, and quick approach for synthesizing citric acid coated manganese ferrite (MnFe_2O_4) nanoparticles through chemical co-precipitation with 1 M NaOH as an oxidative solution. The citric acid coated MnFe_2O_4 nanoparticles were studied by powder X-ray diffraction, Fourier transform infrared spectroscopy, and scanning electron microscopy. The powder X-ray diffraction results confirm the spinel structure of MnFe_2O_4 based on face centred cubic lattice parameters. The Fourier transform infrared spectroscopy results confirm the vibrational modes of citric acid coated MnFe_2O_4 . The scanning electron microscope results of the as synthesised citric acid coated MnFe_2O_4 product had a spherical form with an average diameter of 20 nm. The electrochemical properties of MnFe_2O_4 nanoparticles were studied using cyclic voltammetry, charge-discharge, and electrochemical impedance spectroscopy using 1M NaOH as a electrolyte. Citric-acid coated MnFe_2O_4 nanoparticles shows pseudo-capacitance behaviour properties and delivers a specific capacitance value of about 381 F g^{-1} at 1 A g^{-1} specific current with 15% retention rate at high specific currents. The specific capacitance remained at 92% after 10,000 cycles at a specific current of 2 A g^{-1} which is clearly showed.

Keywords

Rapid Synthesis, MnFe_2O_4 , Citric Acid, Nanoparticles, Supercapacitors

1. Introduction

The next generation need eco-friendly and efficient energy storage systems for a variety of uses, including hybrid electric vehicles and smartphones [1]. Due to poor conductivity in batteries, they limit in output voltage, energy, and power density. To overcome, supercapacitors play a major role in maximum energy storage than capacitors and high-power

density than batteries [2]. Supercapacitors have limited surface area, making it difficult to obtain maximum energy storage capacity. Many scientific research communities are concentrating on developing acceptable materials for high-energy storage devices with maximum power delivery. Supercapacitors are a potential device for energy storage due

*Corresponding author: vishnuvardhan.p@srec.ac.in (Palem Vishnu Vardhan)

Received: 18 September 2024; **Accepted:** 11 October 2024; **Published:** 31 October 2024



Copyright: © The Author (s), 2024. Published by Science Publishing Group. This is an **Open Access** article, distributed under the terms of the Creative Commons Attribution 4.0 License (<http://creativecommons.org/licenses/by/4.0/>), which permits unrestricted use, distribution and reproduction in any medium, provided the original work is properly cited.

to their high power, low equivalent series resistance, and extraordinary cycle life [3]. Electrochemical supercapacitor performance is primarily governed by a variety of parameters, including electrode material surface, morphology, current collector, separator, and electrolyte concentrations etc., [4]. Nanomaterials have unique geometries that significantly impact electrochemical activity. [5]. Supercapacitors are typically made of three types of materials: carbon-based, which store charge through a non-faradic reversible process, metal based and polymer based, stores charge through a pseudo-faradic redox reaction with their respective derivatives at electrode/electrolyte interface [6].

Among metal oxides, ruthenium, manganese, and iron are the most intensively studied due to their ease of preparation, low cost, earth abundant, ecofriendly, valance states, spinel structure and large-scale production [7]. Similarly, spinel ferrite nanocrystals have gained popularity because to their high surface-to-volume ratio and size-dependent characteristics, prompting several studies on their synthesis. These factors influence the physical and chemical properties. Magnetite and spinel ferrite nanocrystals are significant inorganic nanomaterials with unique electronic, optical, electrical, magnetic, and catalytic capabilities that differ from their bulk counterparts. Spinel ferrites have the structure AB_2O_4 , with A and B representing tetrahedral and octahedral cation sites, and O indicating the oxygen anion site [8]. Manganese ferrite ($MnFe_2O_4$) nanoparticles play a significant role in various magnetic applications [9]. Manganese ferrite nanoparticles' qualities depend on their micro-structural characteristics, including particle size and shape, which can be controlled during production. Spinel manganese ferrite nanocrystals can be prepared using a variety of processes, including sol-gel, co-precipitation, reverse micelles, and hydrothermal procedures [10].

In this study, we synthesized $MnFe_2O_4$ nanoparticles to achieve high capacitance, operating voltage, and rate performance in supercapacitors. Herein, we use a rapid, facile, and scalable chemical co-precipitation approach to synthesise $MnFe_2O_4$ nanoparticles. $MnFe_2O_4$ nanoparticles exhibited specific capacitance (SC) of 381 F g^{-1} in NaOH aqueous solutions at a high loading level of approximately 1.0 mg cm^{-2} . The SC demonstrated robust rate performance, excellent retention at higher loading levels, and long-lasting cycling stability over 10,000 cycles.

2. Experimental

Merck Specialties Private Limited, India has supplied $MnCl_2 \cdot 6H_2O$ (99%), $FeCl_3 \cdot 9H_2O$ (98%), KOH (98%), 1-methyl-2-pyrrolidone (NMP), and NaOH (98%). Sigma-Aldrich provided both PVDF and conductive carbon. Hayman provided 99.9% ethanol, while distilled water was purified using a Millipore purifier from Merck in India.

$MnFe_2O_4$ was produced by the co-precipitation technique employing with 0.5 M of $MnCl_2 \cdot 6H_2O$ as a manganese supply, 0.5 M of $FeCl_3 \cdot 9H_2O$ as an iron supply and 0.5 M of citric acid as a template precursor. All precursors were taken in a 200 ml beaker and then stirred for 5 h. The mixture of $MnCl_2 \cdot 6H_2O$ and $FeCl_3 \cdot 9H_2O$ (in the ratio 1: 2) was heated to 80°C with steady stirring. Citric acid is added steadily to the above mixture to obtain sustain coating. Here, Sodium hydroxide, NaOH, was utilized as a reduction agent. After reaching 80°C , steadily add 1 M NaOH solution until the pH hits 14 (base nature). Optimizing the concentrations of precursor solutions and reducing agent resulted in nanoscale particles. After obtaining the powder, it was thoroughly cleaned with water and ethanol to eliminate contaminants and unreacted materials. The brown precipitate was separated and dried in a hot air oven at 80°C for 12 hours.

The X-ray diffraction pattern was captured over a 2θ range of 20 – 60° with a step size of 0.01° with Cu $K\alpha$ ($\lambda = 1.54178 \text{ \AA}$). FTIR spectra were recorded using the Spectrum One Spectrometer. The morphology of the produced powder was examined using cold field emission scanning electron microscopy (JSM 6701F, JEOL, Japan).

To investigate the capacitance properties of $MnFe_2O_4$, electrodes were created by depositing a slurry on stainless steel foil and drying under vacuum at 120°C . The coating and drying procedures were repeated to achieve a loading level of $\sim 1 \text{ mg cm}^{-2}$. Slurry was made by combining electroactive material ($MnFe_2O_4$), super P carbon black (conductive additive), and polyvinylidene fluoride (binder) in a weight ratio of 7: 2: 1, followed by a few drops of N-methylpyrrolidone. Capacitance properties were measured with three electrodes ($MnFe_2O_4$ coated SS-foil as working electrode, Pt wire as counter electrode, and saturated Ag/AgCl as reference electrode). Electrochemical studies were performed utilizing a Autolab Version 1.2 potentiostat/galvanostat system.

3. Physiochemical Characterization

The powder X-ray diffraction pattern (Figure 1) indicates the presence of crystalline $MnFe_2O_4$, which is consistent with the database (PCPDFWIN No. 89-2807). To capture diffraction patterns, utilized a 2θ range of 20 to 60° with a $5^\circ/\text{min}$ period. Scherrer's formula yielded a crystallite size of 20.23 nm . The results confirm the synthesis of nano-crystalline $MnFe_2O_4$ particles. FTIR analysis have been used to better understand the structural configuration of the synthesized sample and shown in the Figure 2. The absorption peaks at 495 , 691 , 1620 and 1396 cm^{-1} indicate the intrinsic stretching vibrations of M-O (metal-oxide) octahedral and tetrahedral sites, C=O ($\nu_{\text{C=O}}$) and asymmetric stretching of C=O attributable to spine shaped $MnFe_2O_4$ coated with the citric acid [11].

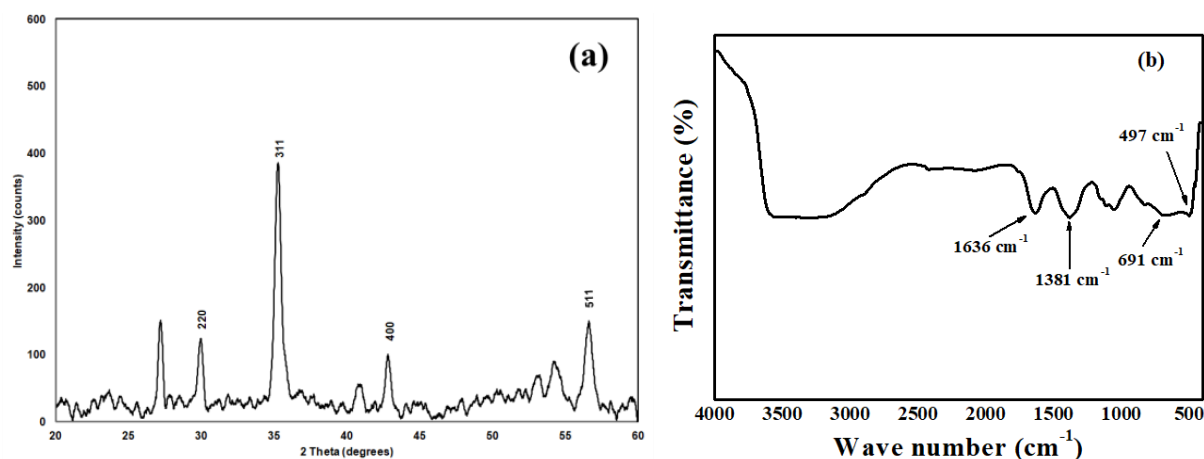


Figure 1. (a) PXRD and (b) FTIR of citric acid coated MnFe_2O_4 nanoparticles.

The scanning electron microscopy (SEM) of the produced powder (Figure 2a and Figure 2b) reveals spherical shaped nanoparticles ranging from 11.32 to 24 nm, with an average size of 20 nm. The produced powder also contains a few nanowires size ranging from 50 to 120 nm, with average size of 75 nm.

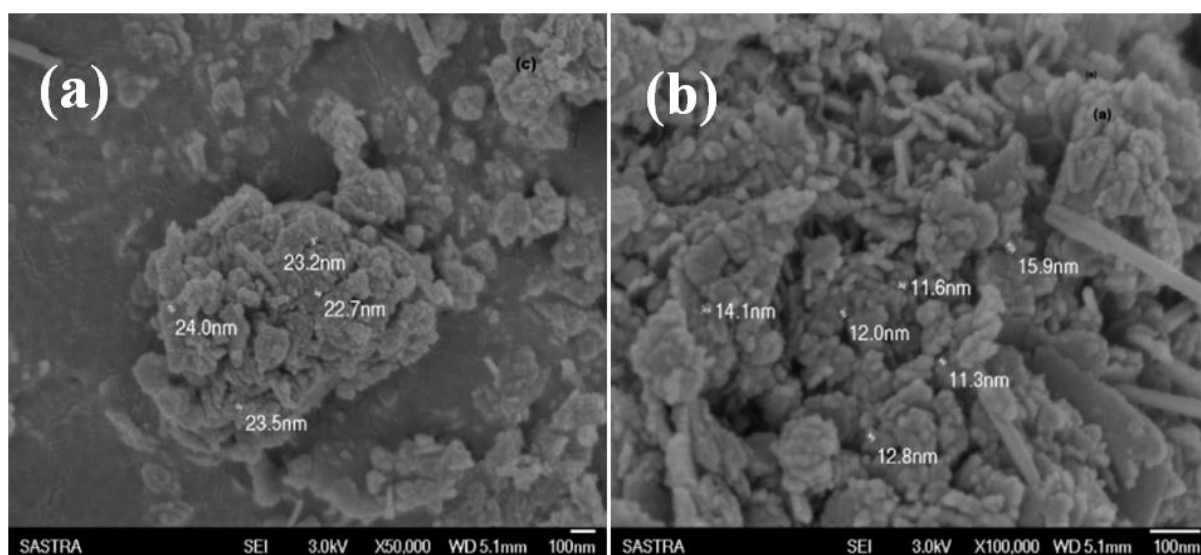


Figure 2. (a) Low resolution and (b) high resolution micrographs of citric acid coated MnFe_2O_4 nanoparticles.

4. Electrochemical Characterization

In Figure 3a & 3b, Cyclic voltammetry (CV) and Galvanostatic charge/discharge (GCD) measurements were performed using a typical three-electrode technique in 1M NaOH electrolyte. Here, stainless steel foil is used as working electrode, Platinum electrode is used as counter electrode and Hg/HgO electrode is used as reference electrode. The CV profile (Figure 3a) shows a working potential range of 0 to 1 V vs. Hg/HgO electrode, which is ascribed to the synergistic contributions of Fe and Mn metal ions. The obtained CV profile perfectly matches with the significant feature of pseudo capacitance behaviour [12-15].

In Figure 3b, shows the GCD profile of the MnFe_2O_4 electrode in 1M NaOH electrolyte at various specific currents. Linear increase in the potential and linear decrease in the potential is observed while a specific current applied. This also behaviour also supports the CV profile, where it shows significant feature of pseudo capacitance behaviour as well. The authorized method is used to determine specific capacitance (SC) values during galvanostatic charge-discharge cycles [16]. The SC value of 381 F g⁻¹ for citric acid-coated MnFe_2O_4 nanoparticles with a load level of 0.5 mg cm⁻² at a specific current of 1 A g⁻¹ in 1M NaOH electrolyte. The literature suggests that MnFe_2O_4 may exhibit two pairs of redox peaks (Fe and Mn), indicating a quick and reversible redox process that can be stated as follows in eq (1) and eq (2).

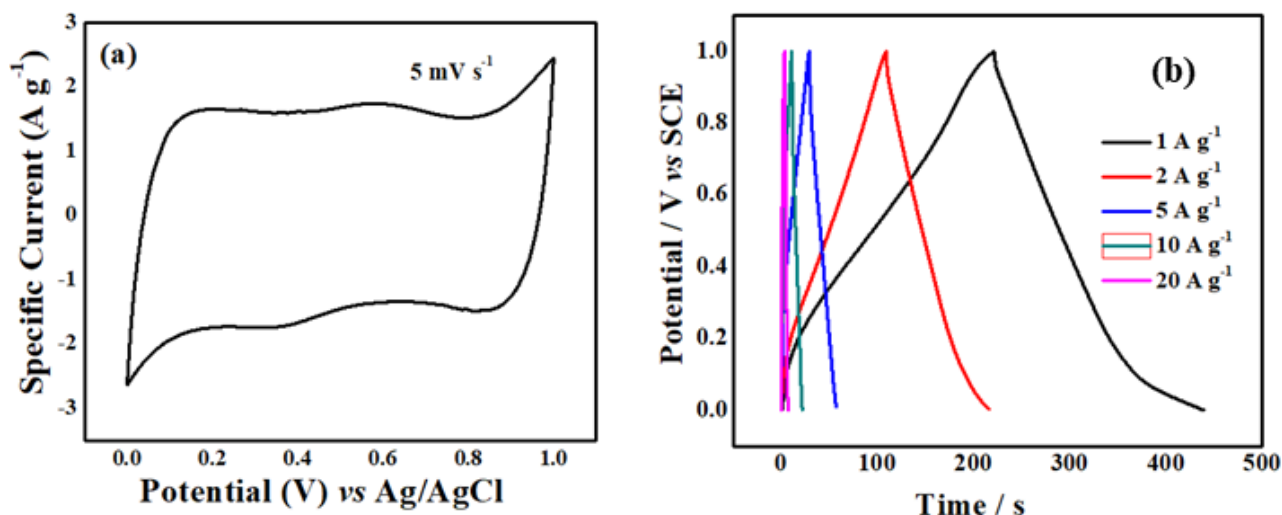


Figure 3. (a) CV recorded at scan rate of 5 mV s^{-1} , and (b) GCD recorded at various specific currents of citric-acid coated MnFe_2O_4 in 1 M of NaOH electrolyte.

Figure 4a shows that the area under the CV profile grows linearly with increase in the scan rate, indicating that even at higher scan rates, maximal electrode active surfaces are accessible with adequate electrical conductivity. In Figure 4b, shows rate performance of citric-acid coated MnFe_2O_4 nano-

particles. The rate performance of citric-acid coated MnFe_2O_4 nanoparticles were tested at various specific current varies from 1 to 20 A g^{-1} in 1M NaOH electrolyte. SC drops to 15% of its initial value as specific currents increase due to material deterioration and increased internal resistance.

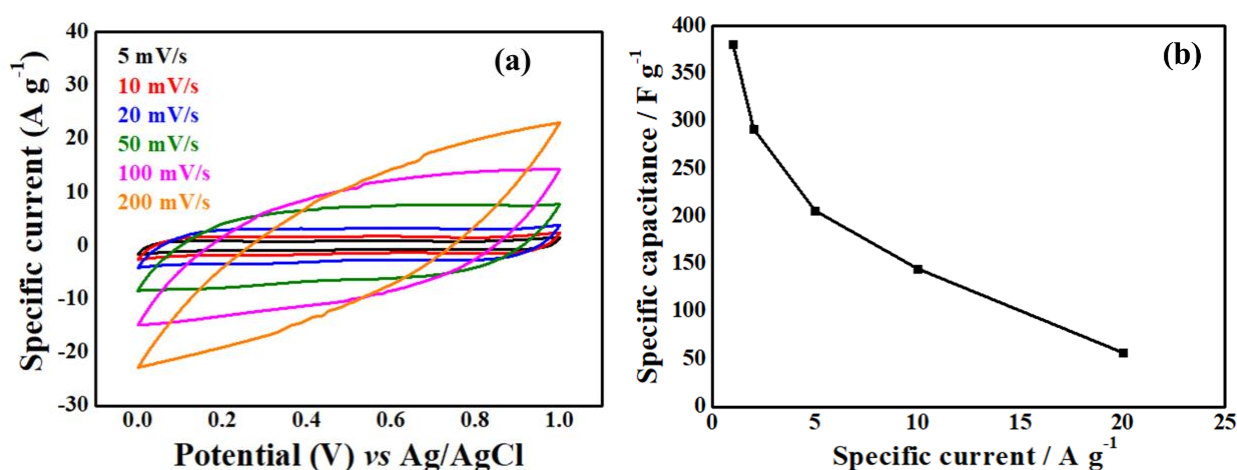


Figure 4. (a) CV recorded at various scan rates, and (b) rate performance of citric-acid coated MnFe_2O_4 recorded at various specific currents in 1 M of NaOH electrolyte.

In Figure 5, shows EIS spectra of citric-acid coated MnFe_2O_4 nanoparticles along with the data matched using an equivalent circuit, which is shown inset. The high-frequency intercept with the real axis represents the electrolyte (R_s), whereas the clearly defined semicircle represents the interfa-

cial charge-transfer resistance (R_{ct}). Ionic diffusion (Warburg impedance, W) in the material leads to the linear low-frequency zone. The parameters that were acquired by fitting EIS from 1M NaOH electrolyte are as follows, $R_s = 12.7\Omega$, $R_{ct} = 4.9\Omega$.

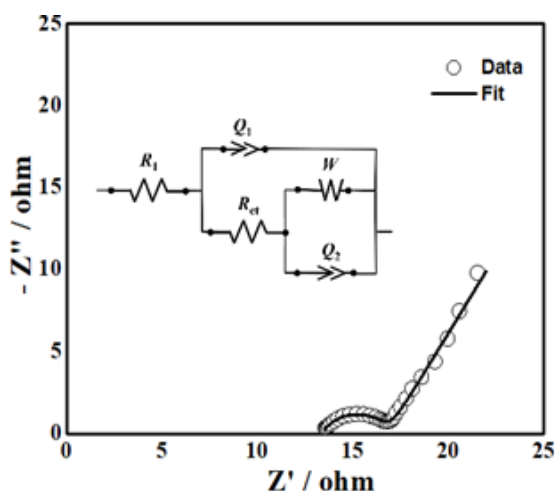


Figure 5. Nyquist plot of EIS spectrum and corresponding equivalent circuit used for fitting EIS spectrum was given in inset of citric-acid coated MnFe_2O_4 nanoparticles in 1M NaOH electrolyte.

The citric-acid coated MnFe_2O_4 nanoparticles are subjected to extended GCD life cycles at 2 A g^{-1} specific current to assess the cycling stability of the material and shown in the Figure 6. Over 10,000 cycles, SC of citric-acid coated MnFe_2O_4 nanoparticles sustains 92% in 1M NaOH electrolyte.

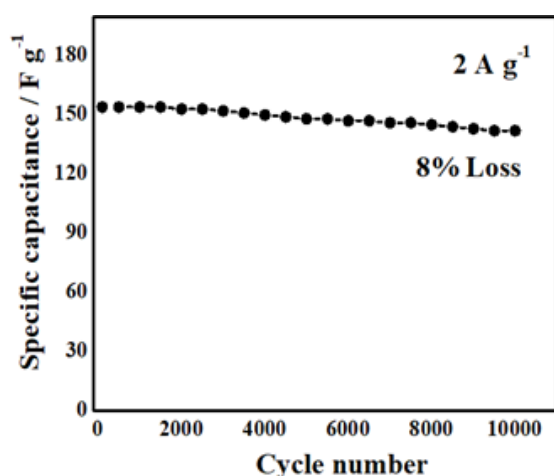


Figure 6. Nyquist plot of EIS spectrum and corresponding equivalent circuit used for fitting EIS spectrum was given in inset, and (b) cycle life of citric-acid coated MnFe_2O_4 nanoparticles in 1M NaOH electrolyte.

5. Conclusion

MnFe_2O_4 nanoparticles were synthesized via a rapid, scalable co-precipitation process, and its superior capacitive storage performance was proven. In NaOH electrolyte, high specific capacitance of 381 F g^{-1} was attained at a specific current of 1 A g^{-1} . The shape and size of the material discovers the high specific capacitance. MnFe_2O_4 nanoparticles has a

excellent rate capacity and stable cycle life that are equivalent to those previously reported for MnFe_2O_4 nanoparticles.

Abbreviations

MnFe_2O_4	Manganese Ferrite
$\text{MnCl}_2 \cdot 6\text{H}_2\text{O}$	Manganese Chloride Tetrahydrate
$\text{FeCl}_3 \cdot 9\text{H}_2\text{O}$	Ferric Chloride Nonahydrate
CV	Cyclic Voltammogram
GCD	Galvanostatic Charge/Discharge
EIS	Electrochemical Impedance Spectroscopy

Acknowledgments

The authors wish to acknowledge, The Management, Sri Ramakrishna Engineering College for providing the infrastructure and instrument facilities, and I acknowledge financial support (DST/TDT/TDP/-06/2022) from Department of Science and Technology, Government of India.

Author Contributions

Palem Vishnu Vardhan: Conceptualization, Investigation, Project administration, Resources, Supervision, Validation, Writing – original draft, Writing – review & editing

Pichumani Moorthi: Funding acquisition, Resources, Validation, Writing – review & editing

Palanivel Nihitha: Data curation, Resources, Writing – original draft, Writing – review & editing

Sivakumar Kamalikka: Data curation, Resources, Writing – original draft, Writing – review & editing

Karthikeyan Surya: Data curation, Investigation, Writing – original draft, Writing – review & editing

Conflicts of Interest

The authors declare no conflicts of interest.

References

- [1] T. Kozawa, T. Murakami, M. Naito, Insertion of lattice strains into ordered $\text{LiNi}_{0.5}\text{Mn}_{1.5}\text{O}_4$ spinel by mechanical stress: a comparison of perfect versus imperfect structures as a cathode for Li-ion batteries, *J. Power Sources* 320 (2016) 120-126. <http://dx.doi.org/10.1016/j.jpowsour.2016.04.086>
- [2] F. Tao, Y. Q. Zhao, G. Q. Zhang, H. L. Li, Electrochemical characterization on cobalt sulfide for electrochemical super-capacitors, *Electrochem. Commun.* 9 (2007) 1282 – 1287. <http://dx.doi.org/10.1016/j.elecom.2006.11.022>
- [3] A. Burke, R&D considerations for the performance and application of electrochemical capacitors, *Electrochim. Acta* 53 (2007) 1083–1091. <https://doi.org/10.1016/j.electacta.2007.01.011>

- [4] H. Su, H. Zhang, F. Liu, F. Chun, B. Zhang, X. Chu, H. Huang, W. Deng, B. Gu, H. Zhang, X. Zheng, M. Zhu, W. Yang, High power supercapacitors based on hierarchically porous sheet-like nanocarbons with ionic liquid electrolytes, *Chem. Eng. J.* 322 (2017) 73–81.
<http://dx.doi.org/10.1016/j.cej.2017.04.012>
- [5] L. J. Xie, J. F. Wu, C. M. Chen, C. M. Zhang, L. Wan, J. L. Wang, Q. Q. Kong, C. X. Lv, K. X. Li, G. H. Sun, A novel asymmetric supercapacitor with an activated carbon cathode and a reduced graphene oxide-cobalt oxide nanocomposite anode, *J. Power Sources* 242 (2013) 148–156.
<http://dx.doi.org/10.1016/j.jpowsour.2013.05.081>
- [6] H. Y. Lee, J. B. Goodenough, Supercapacitor behaviour with KCl electrolyte, *J. Solid State Chem.* 144 (1999) 220–223.
<https://doi.org/10.1006/jssc.1998.8128>
- [7] B. Sljukic, C. E. Banks, R. G. Compton, Iron oxide particles are the active sites for hydrogen peroxide sensing at multi-walled carbon nanotube modified electrodes, *Nano Lett.* 6 (2006) 1556–1558, <http://dx.doi.org/10.1021/nl060366v>
- [8] B. Bashir, W. Shaheen, M. Asghar, M. F. Warsi, M. A. Khan, S. Haider, I. Shakir, M. Shahid, Copper doped manganese ferrites nanoparticles anchored on graphene nano-sheets for high performance energy storage applications, *J. Alloys Compd.* 695 (2017) 881–887. <http://dx.doi.org/10.1016/j.jallcom.2016.10.183>
- [9] P. Vishnu Vardhan, K. S. Suganthi, S. Manikandan and K. S. Rajan, Nanoparticle Clustering Influences Rheology and Thermal Conductivity of Nano-Manganese Ferrite Dispersions in Ethylene Glycol and Ethylene Glycol-Water Mixture, *Nanosci. Nanotechn. Lett.*, 6 (2014) 1095–1101.
<https://doi.org/10.1166/nnl.2014.1884>
- [10] L. Liu, J. Lang, P. Zhang, B. Hu, X. Yan, Facile synthesis of Fe₂O₃ nano-dots@ Nitrogen-doped graphene for supercapacitor electrode with ultralong cycle life in KOH electrolyte, *ACS Appl. Mater. Interfaces* 8 (2016) 9335–9344,
<http://dx.doi.org/10.1021/acsami.6b00225>
- [11] V. Aishwarya, K. S. Suganthi, K. S. Rajan, Transport properties of nano manganese ferrite–propylene glycol dispersion (nanofluids): new observations and discussion, *J. Nanopart. Res.* 15, (2013) 1774.
<https://doi.org/10.1007/s11051-013-1774-3>
- [12] B. E. Conway, *Electrochemical Supercapacitors*, Kluwer Academic/Plenum Press, New York, Scientific Fundamentals and Technological Applications, 1999.
- [13] B. E. Conway, Transition from “supercapacitors” to “battery” behaviour in electrochemical energy storage, *J. Electrochem. Soc.* 138 (1991) 1539–1548,
<https://doi.org/10.1149/1.2085829>
- [14] A. Burke, Ultracapacitors: why, how, and where is the technology, *J. Power Sources* 91 (2000) 37–50,
[https://doi.org/10.1016/S0378-7753\(00\)00485-7](https://doi.org/10.1016/S0378-7753(00)00485-7)
- [15] A. Burke, R&D considerations for the performance and application of electrochemical capacitors, *Electrochim. Acta* 53 (2007) 1083–1091,
<https://doi.org/10.1016/j.electacta.2007.01.011>
- [16] S. Devaraj, H.Y. Liu, P. Balaya, MnCO₃: a novel electrode material for supercapacitors, *J. Mater. Chem. A* 2 (2014) 4276–4281, <https://doi.org/10.1039/C3TA14174H>